ORIGINAL RESEARCH

Taxifolin, Extracted from Waste *Larix olgensis* Roots, Attenuates CCl₄-Induced Liver Fibrosis by Regulating the PI3K/AKT/mTOR and TGF-β1/ Smads Signaling Pathways

Xinglong Liu[1]
Wencong Liu[1,2]
Chuanbo Ding[1]
Yingchun Zhao[1]
Xueyan Chen[1]
Dong Ling[1]
Yinan Zheng[1]
Zhiqiang Cheng[3]

[1]College of Chinese Medicinal Materials, Jilin Agricultural University, Changchun 130118, People's Republic of China; [2]State Local Joint Engineering Research Center of Ginseng Breeding and Application, Changchun 130118, People's Republic of China; [3]College of Resources and Environment, Jilin Agricultural University, Changchun 130118, People's Republic of China

Purpose: Taxifolin is a kind of dihydroflavone and is usually used as a food additive and health food for its antioxidant, anti-inflammatory, and anti-tumor activities. The purpose of this research is to probe into the hepatoprotective activity and the molecular mechanism of taxifolin.

Materials and Methods: The liver fibrosis model was established by intraperitoneal injection of 5 mL/kg body weight of CCl₄ (20% CCl₄ peanut oil solution), and taxifolin was dissolved with 0.9% physiological saline and administered intragastrically to mice.

Results: The results indicated that CCl₄-induced significantly increased the serum alanine aminotransferase (ALT) and aspartate aminotransferase (AST) in mice. Histopathological examination showed severe hepatocyte necrosis and hepatic tissue lesion. Immunohistochemical staining and rt-PCR analysis demonstrated that the expressions of inducible nitric oxide synthetase (iNOS), cyclooxygenase-2 (COX-2), IL-1β, IL-6, and TNF-α were increased. These changes were significantly reversed when treated with taxifolin. In addition, TUNEL staining and Bcl-2/Bax pathway confirmed that taxifolin significantly inhibited hepatocyte apoptosis. Besides, the research confirmed that taxifolin also inhibited the activation of hepatic stellate cells and the production of extracellular matrix (ECM) by regulating PI3K/AKT/mTOR and TGF-β1/Smads pathways.

Conclusion: Taxifolin inhibited inflammation, and attenuated CCl₄-induced oxidative stress and cell apoptosis by regulating PI3K/AKT/mTOR and TGF-β1/Smads pathways, which might in part contributed to taxifolin anti-hepatic fibrosis, further demonstrating that taxifolin may be an efficient hepatoprotective agent.

Keywords: taxifolin, liver fibrosis, PI3K/AKT/mTOR pathway, TGF-β1/Smads, inflammation, apoptosis

Introduction

Numerous liver grievances, such as hepatitis epidemiologic infection, alcohol intake, cholestasis, and non-alcoholic steatohepatitis are source liver fibrosis, which is a self-motivated wound curative process.[1] The superfluous production of extracellular matrix (ECM) constituents is characteristic of liver fibrosis, which in turn interrupts the normal liver construction and function.[2,3] Liver cirrhosis and hepatic carcinoma occur due to insistent liver fibrosis and absence of treatment. Furthermore, a substantial amount of sickness and death in patients takes place due

Correspondence: Wencong Liu
College of Resources and Environment, Jilin Agricultural University, #2888 Xincheng Street, Changchun 130118, People's Republic of China
Tel +86 138 0446 0499
Email jwlw6803@126.com

to liver fibrosis, and an operative remedy is not yet obtainable. Thus, in order to avert or cure liver fibrosis, there is a crucial petition for evolving new medicines.[4,5] The mechanisms of liver fibrosis have been extensively examined in current years. It has been proved that a mass of reactive oxygen species (ROS) is produced during expansion and evolution of liver fibrosis, which leads to lipid peroxidation and hepatocyte necrosis, and then leads to oxidative stress injury and activation of hepatic stellate cells (HSCs), and the activation of HSCs triggers and secretes a large amount of ECM.[6,7] Overexpression of ECM and alpha-smooth muscle actin (α-SMA) eventually leads to complications such as liver fibrosis and liver failure.[1,8] Numerous studies have confirmed that HSCs activation and ECM synthesis are meticulously related with PI3K/AKT/mTOR and TGF-β/Smads signaling pathways, and the PI3K/AKT/mTOR signaling pathway was convinced this result by pharmacological and genetic approaches.[8] Besides this PI3K/AKT/mTOR pathway, TGF-β1 stimulates Smads pathways to display its biological activities. It is illustrated that TGF-β1 applies its biological possessions by motivating downstream mediators Smad2 and Smad3.[9] Smads also act as signal integrators and interrelate with further signaling pathways, such as the MAPK and NF-κB signaling pathways.[10] Consequently, the PI3K/AKT/mTOR and TGF-β/Smads signaling pathways play an important role as main healing targets in order to handle liver fibrosis. In addition to these pathways, the Bcl-2/Bax signaling pathway correspondingly shows a major part by regulating cell apoptosis and improves the expansion of liver fibrosis. Insistent liver apoptosis enhance liver fibrosis, while amending the Bcl-2/Bax signaling pathway might constrain hepatocyte apoptosis and diminish liver fibrosis.[11,12] Bcl-2 anti-apoptotic molecules exist as protectors of the mitochondrial pathway of cell apoptosis.

Taxifolin (3,3′,4′,5,7-pentahydroxiflavanon, TAX) is a famous flavanol compound,[13] mainly from pine plants such as larch and douglas fir.[14] TAX is usually used as a natural antioxidant additive in the food industry.[15] The European Commission (EU) issued regulation no 2015/2283 authorizing taxifolin-rich extract to be put on the EU market as a new food ingredient on March 21, 2018. In recent years, increasing research has proved that TAX has more positive effects on health, such as anti-oxidation, anti-tumor, anti-radiation, and anti-viral pharmacological activities.[16–22] Meanwhile, TAX prevents diabetic cardiomyopathy by inhibiting oxidative stress, activating JAK2/

STAT3 cascade activation and reducing angiotensin II production.[23] In addition, TAX treats cardiac hypertrophy and fibrosis by inhibiting the overproduction of ROS, ERK1/2, JNK1/2, and Smad signaling pathways.[24] In addition, TAX has also been shown to have potent anti-proliferative effects on mouse fibroblasts and human breast cancer cells.[25] However, the effect of TAX on liver fibrosis and the associated molecular mechanisms is unclear.

Larix olgensis resources in China are mainly distributed in the northeast. *Larix olgensis* trunk is used in industrial production, which is an important forestry resource. However, *Larix olgensis* roots are discarded as waste, which not only leads to a low utilization rate of resources, but also occupies a lot of storage space. In addition, rotten roots cause environmental pollution. In this study, we obtained taxifolin-rich extract from a large number of abandoned Larch roots, in order to explore the preventive effect of TAX on long-term CCl$_4$-induced liver fibrosis and its molecular mechanism in mice. It can not only obtain taxifolin with high biological activity, but also improve the utilization rate of resources.

Materials and Methods
Chemicals and Reagents

The reference standard of taxifolin was bought from the National Institutes for Food and Drug Control, batch no: 111,816–201,102, with purity of 98.0%. CCl$_4$ was bought from Shenzhen Xunye Chemical (purity≥99.5%; Shenzhen, China). The commercial assay kits of aspartate aminotransferase (AST), alanine aminotransferase (ALT), total bilirubin (TBIL), glutathione (GSH), glutathione disulfide (GSSG), superoxide dismutase (SOD), malondialdehyde (MDA), interleukin-1β (IL-1β), interleukin-6 (IL-6), tumor necrosis factor-α (TNF-α), and hematoxylin-eosin (H&E) were purchased from Nanjing Jiancheng Bioengineering Research Institute (Nanjing, China). Enzyme linked immunosorbent assay (ELISA) kits of mouse transforming growth factor-β1 (TGF-β1) was delivered by R&D systems (Minneapolis, MN, USA). Immunofluorescence staining kit was delivered by the Boster Biological Technology Co. Ltd (Wuhan, China). The antibody of rabbit monoclonal anti-muscle inducible nitric oxide synthase (iNOS), cyclooxygenase-2 (COX-2), α-smooth muscle actin (α-SMA), Smad3, anti-TGF-β1, Cytochrome P450 E1 (CYP2E1), and HRP-conjugated anti-mouse IgG were purchased from Abcam (Cambridge, UK). Anti-B-cell lymphoma-2 (Bcl-2), anti-B-associated X(Bax), anti-cleaved caspase-3, anti-caspase

-3, protein kinase B(Akt), p-Akt, mammalian Target of rapamycin (mTOR), p-mTOR, Phosphatidylinositol 3-kinase (PI3K), p-PI3K, and β-actin monoclonal antibodies were bought from Cell Signaling Expertise (Danvers, MA). All additional chemicals were bought from Beijing Chemical Factory (Beijing, China).

Preparation for Taxifolin

Larch roots were taken from Changbai Mountain Forest Farm in Jilin Province, China. The dust and impurities were washed away, then the roots were crushed into wood chips, and used through a 30-mesh sieve. Weigh 200 g of wood chips, use ethanol heating and reflux method, add 2,000 mL of 90% ethanol at a material–liquid ratio of 1:10 (g/mL), extract at 90°C for 3 hours, repeat three times, and then filter and combine the extracts. It was concentrated under reduced pressure, then dissolved in hot water at 80°C, and quickly crystallized at 4°C. After that, it was repeatedly recrystallized and dried to obtain the light yellow powder of taxifolin-rich extract.

Determination of Taxifolin by HPLC-UV/ESI-MS

The dried taxifolin-rich extract was precisely weighed (1.00 g), and dissolved in 100 mL of methanol:water (2:3), and filtered using a 0.22 μm microporous filter membrane, then analyzed by HPLC.

Taxifolin-rich extract was analyzed on Waters HPLC system (Waters, e2695, USA) with a UV detector. Samples were separated on COSMOSIL C18-PAQ column (4.6 mm×250 mm, 5 μm). The column temperature was set to 30°C. The detection wavelength was set to 288 nm, and the mobile phase was: methanol:water (40:60) with a flow rate of 1.0 mL/min. Taxifolin was confirmed through comparing the retention time of the sample with the reference standard.

The HPLC-UV system was connected to the MS detector and subjected to mass spectrometry (ESI-MS) using a positive electrospray ion fragmentation pattern. The capillary potential was 4.0 kV, the drying gas temperature was 300°C, and the flow rate was 10.0 L/min, and the atomizer pressure was 45 psig. The total ion chromatogram obtained in ESI positive mode was 150–1,000 m/z. It was finally determined as TAX.

Animals and Experimental Plan

The Changchun YISI Experimental Animal Co., Ltd (Certificate of Quality is No. SCXK (JI)-2016-0003) (Changchun, China) delivered 60 fully-grown male ICR mice (6–8 weeks old; weight 22–25 g). The mice were placed at a precise pathogen-free climate in a moisture-controlled atmosphere and 12 hours light-dark cycle. Food and water were freely accessed. The experiments were conducted in accordance with the National Institutes of Health Guide for Laboratory Animals Care and Use and the Laboratory Animal Management Committee of Jilin Agricultural University, and approved by the Animal Investigational Morals Committee of Jilin Agricultural University, with ethics approval number: 2019–08-28-002.

After acclimation for 1 week, mice were distributed haphazardly into six groups (n=10 for each set) such as mentioned here: normal group, CCl$_4$ model group (only treatment with CCl$_4$), positive control group (treatment with colchicine), the 20 mg/kg TAX group, the 40 mg/kg TAX group, and the 80 mg/kg TAX group. An advanced hepatic fibrosis model was recognized by inducing CCl$_4$ with an adjusted amount, as explained in the procedure (Figure 1A). All mice received 5 mL/kg CCl$_4$ intraperitoneal (20% CCl$_4$ peanut oil solution) two times a week for 8 weeks to induce liver fibrosis, except those in the normal group. After 4 weeks of intraperitoneal injection of CCl$_4$, the positive drug group was given 0.2 mg/kg colchicine, and the TAX groups were given doses of 20, 40, and 80 mg/kg body weight, respectively, once daily for 4 weeks. Mice in the normal group were injected with the same amount of peanut oil. The weight of alive mice was calculated and then these mice were anesthetized with pentobarbital sodium (Shanghai Beizhuo Biochemical & Technological Co., Ltd., Shanghai, China) at the end of 8 weeks. Serum was sequestered from blood through centrifugation (1000×g for 15 minutes) after accumulating the blood samples from the abdominal aorta. Liver sections were preserved with 10% formaldehyde, and remaining liver segments were preserved at −80°C for additional experiments.

Biochemical Analysis

By conferring to industrialist's procedure, and consuming a clinical automatic analyzer (Hitachi, Japan) and a commercial reagent kit (Roche Diagnostic, Mannheim, Germany), levels of Serum ALT, AST, and TBIL were quantified. Hepatic quantity was quantified conferring to the company's protocol with hydroxyproline detection kit (Sigma-Aldrich, St. Louis, Mo, USA). GSH, GSSG, SOD, MDA, IL-1β, and TNF-α intensities were quantified via commercial kits (Lipid peroxidation). The quantity of oxidative stress damage was evaluated by the proportions GSH:GSSG. According to the producers' protocols all the processes were accomplished.
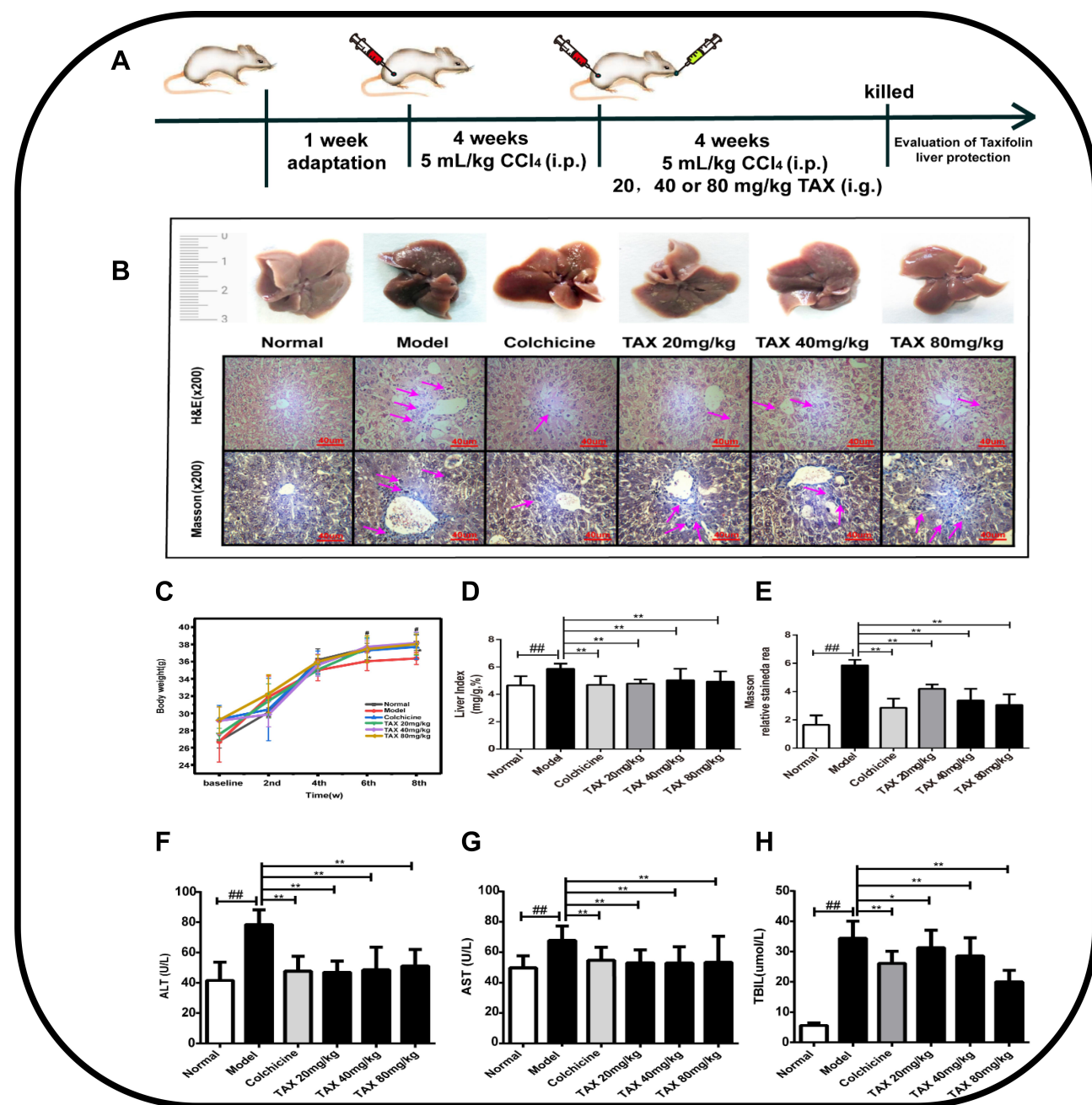
Figure 1 Taxifolin (TAX) mitigates liver injury and fibrosis in mice. (**A**) The experimental process. (**B**) H&E staining of liver tissue, amplification: ×200; Masson staining of liver tissue, amplification: ×200. (**C**) The body weight of mice. (**D**) The liver index mg/g %. (**E**) Masson relative stained area. (**F** and **G**) Level of ALT and AST in the liver of mice. (**H**) TBIL level in serum of mice. Data expressed as mean±SD (n=10). As compared with the normal group, [#]$P<0.05$ indicates a significant difference, [##]$P<0.01$ indicates an extremely significant difference; As compared with the model group, *$P<0.05$ indicates a significant difference, **$P<0.01$ indicates a extremely significant difference.
Abbreviations: TAX, taxifolin; ALT, alanine aminotransferase; AST, aspartate aminotransferase; TBIL, total bilirubin.

Histological Analysis

Liver sections were preserved in 10% formalin, embedded in paraffin, and segmented. For histological examination, liver pieces remained tarnished with H&E. By ensuring the standards, the degree of liver fibrosis was assessed. For the valuation of collagen constituents in the livers, liver segments were tarnished with Masson's trichrome staining. Sections were stained with TUNEL staining assay kit in order to measure apoptosis in the liver tissue. By means of a light microscope and the quantity, one computerized morphometry system fibrotic area was measured (Bio-Rad, Hercules, USA). Histological valuation was done by randomized assortment.

Immunohistological and Immunofluorescence Staining

In order to notice the countenance of iNOS and COX-2, immunohistological examination was done. Briefly, to chunk endogenous peroxidase action liver segments were deparaffinized and treated with 3% H_2O_2, and used citrate buffer antigen retrieval. After cooling, in order to slab non-specific protein assembling segments remained preserved with 5% BSA, then these segments were kept warm with anti-iNOS (1:200) and anti-COX-2 (1:200) overnight at 4° C. In the meantime, liver segments were incubated with PBS alone and established as negative controls. Then they were washed with PBS and kept warm in an incubator with a biotinylated secondary antibody (1:1) and avidin-biotin-peroxidase compound, then tarnished with DAB. All liver segments were detected by microscope (Olympus, Tokyo, Japan).

Preliminary section processing was as shown in immunohistochemistry, and the sections were incubated with CYP2E1 (1:200) at 4°C for 10 hours in immunofluorescence staining. Subsequently, hatched by dye-488 labeling after 12 hours at 37°C. The nuclei of the fixed tissue were re-stained with 4.6-diamino-2-phenylindole (DAPI). At the same time, the degree of immunofluorescence staining was detected by fluorescence microscope (Leica DMILED, Germany), and the optical density analysis was performed using Image-Pro Plus 6.0 software.

Western Blotting Analysis

Using RIPA lysis buffer and phosphatase inhibitor (Sangon Biotech Co., Ltd., Shanghai, China) hepatic tissues were lysed. Thirty micrograms of protein was separated by SDS-polyacrylamide and this was transported on a PVDF membrane after 2 hours treatment with bovine serum albumin (BSA). Using primary antibodies (TGF-β1, α-SMA, Akt, p-Akt, mTOR, p-mTOR, PI3K, p-PI3K, Bax, Bcl-2, caspase 3, and cleaved caspase 3) at 4°C the membranes remained incubated for the whole night. After incubating with equivalent secondary antibodies (β-actin) proteins intensities were analyzed by Emitter Coupled Logic (ECL) substrate (Pierce Chemical Co., Rockford, IL, USA). Quantity One software (Bio-Rad Laboratories, Hercules, USA) was used for examination of the protein band and analyzed by Quantity One (Bio-Rad) according to standard technique.

Real-Time PCR Analysis

Liver sections was regimented by a TL2020 crushing gadget (DHS Life Science & Technology, Beijing, China). Consuming trizol reagent (Invitrogen) subsequent to the procedure given by industrialist, whole RNA was taken from the liver sections. By using rt-PCR intensities of different factors, such Bcl-2, Bax, TGF-β1, α-SMA, matrix metalloproteinase-9 (MMP-9), and tissue inhibitor of metalloproteinase-2 (TIMP-2) were examined. By using the method described earlier, real-time PCR was accomplished.[26] The reference gene used in this process was β-actin. Using cycle threshold (Ct) the countenance intensities were examined and then using the $2^{-\Delta\Delta Ct}$ method stabilized to β-actin appearance. Consequences were obtained from triplicate experiments. Table 1 showed the primer categorizations used in the PCR reactions.

Statistical Analysis

All the displayed data are average±SD. Statistical significance was determined by one-way analysis of variance (ANOVA). Then use SPSS18.0 software to carry out the least significant difference (LSD) multiple comparison test, where $P<0.05$ is considered significant. Statistical graphs were produced via software of GraphPad Prism 6.0.4 software (GraphPad Software, Inc, San Diego, USA).

Table 1 Fluorescence Quantification Primer Sequence

Gene	Primer Sequencing (Forward and Reverse)	
TGF-β1	Forward	5'-TACGGCAGTGGCTGAACCAA-3'
	Reverse	5'-CGGTTCATGTCATGGATGGTG-3'
α-SMA	Forward	5'-CTTATTGGCCTTGCCTTGCT-3'
	Reverse	5'-ACCACAGTTGTCACGGCACT-3'
MMP-9	Forward	5'-GCCCTGGAACTCACACGACA-3'
	Reverse	5'-TTGGAAACTCACACGCCAGAAG-3'
TIMP-2	Forward	5'-TGCAAGATCACTCGCTGTCC-3'
	Reverse	5'-CTCTTGATGCAGGCGAAGAA-3'
Bcl-2	Forward	5'-ATGTGTGTGGAGAGCGTCAACC-3'
	Reverse	5'-GAGCAGAGTCTTCAGAGACAGCC-3'
Bax	Forward	5'-ATTGCCGCCGTGGACACAGA-3'
	Reverse	5'-ATGGTGAGTGAGGCGGTGAG-3'
β-actin	Forward	5'-GTGCTATGTTGCTCTAGACTTCG-3'
	Reverse	5'-ATGCCACAGGATTCCATACC-3'

Abbreviations: TGF-β1, transforming growth factor-β1; α-SMA, α-smooth muscle actin; Bcl-2, B-cell lymphoma; Bax, B-associated X; MMP-9, matrix metalloproteinase-9; TIMP-2, tissue inhibitor of metalloproteinase 2.

Results
HPLC and MS Analysis of TAX

As taxifolin was extracted by hot reflux method, and its structure had a variety of active phenolic hydroxyl groups (Figure 2A) and had strong antioxidant properties, the purity of taxifolin by HPLC method was 95.0% (Figure 2B).

In short, through the retention time of UV spectroscopy and HPLC, and the ESI-MS m/z observed on the MS system: $[M + H]^+304.2$ (Figure 2C), it was determined that the molecular weight of the compound was 304.2. Matching with the taxifolin reference and previously reported theoretical molecular weight, the obtained sample was determined to be taxifolin.

TAX Mitigates Markers of Hepatic Injury and Fibrosis in Mice

Liver fibrosis model was prepared by CCl$_4$-induced, for exploring the defensive consequence of TAX contrary to chronic liver injury and fibrosis (Figure 1A). As designated by the histopathological examinations, mice injected with CCl$_4$ established noticeable liver fibrosis, which induced lesion characteristic with porous surface and eventually graininess and inflammation were noticeably detected in the liver. This phenomenon was explored by the histopathological examination with H&E staining, with obvious parenchymal injury, inflammatory portal infiltration, and accompanied by a large number of inflammatory cells around the hepatic portal. Moreover, Masson staining was done to evaluate the fibrotic notch by recognizing collagen fibers. In the model group numerous fibroblast-like cells and considerable centrilobular hepatic injury were seen (Figure 1B and E).

Though there was no remarkable variance in the body weight and other organ indexes, long-term and repeated injections of CCl$_4$ caused a significant increase in liver pathological index, which indicated that CCl$_4$ interfered with the metabolic process of the liver and caused continuous inflammatory infiltration in the CCl$_4$ model (Figure 1C and D). In order to further confirm the liver injury by CCl$_4$-induced, we conducted repeated stimulation observations and detected these changes through biochemical indicators. As shown in Figure 1F–H, the intensities of AST, ALT, and TBIL in the model group were increased meaningfully due to CCl$_4$ induction as compared to the normal group. However, TAX handling not only amended the pathological abrasions equated to the model group ($P<0.05$), but also reduced the activity of ALT, AST, and

TBIL. These results were consistent with the results of the positive colchicine-group. According to these, data recommended that TAX showed a shielding influence contrary to CCl$_4$-induced prolonged liver fibrosis in mice.

TAX-Treatment Attenuates CCl$_4$-Induced Oxidative Stress and Inflammation

In order to evaluate the function of TAX on CCl$_4$-induced oxidative stress, the levels of liver MDA, GSH, GSSG, and SOD were assayed with the supernatant of liver homogenate. The intensities of the oxidative stress markers MDA, GSH, GSSG, and SOD were resolute in the liver tissue in order to exhibit the TAX effect on CCl$_4$-induced oxidative stress in mice. MDA is usually used as a biomarker of liver oxidative mutilation and is the product of lipid peroxidation. SOD protect cells against oxidative stress by eliminating detrimental oxygen free radicals. For oxidative stress, GSH is tangled in the enzymatic detoxification reaction. In the liver from CCl$_4$-induced mice, by examining the proportion of GSH to GSSG, the consequence of TAX on the glutathione system was inspected. The results showed that in CCl$_4$-induced groups as equated to the normal group CCl$_4$ have meaningfully raised up the level of MDA, which indicated that CCl$_4$ exerted severe damage on an antioxidant defense system ($P<0.01$), while TAX treatment meaningfully reduced the level of MDA in different degrees ($P<0.05$; Figure 3A). In the meantime, levels of SOD and GSH remained reduced in CCl$_4$-induced livers, though their level was not improved in a dose-dependent manner and TAX handling reestablished the GSH/GSSG ratio ($P<0.05$; Figure 3B–D). Since CYP-mediated biological activation plays an important role in the toxicity of liver fibrosis, the fluorescence intensity of CYP2E1 in CCl$_4$-induced liver fibrosis tissue was examined by immunofluorescence staining in this study. Indeed, the administration of TAX reduced the fluorescence intensity of CYP2E1 (Figure 3E and F). These results indicated to a certain extent that TAX reduced the oxidative stress injury by CCl$_4$-induced.

Moreover, intensities of inflammatory cytokines and biomarkers in serum were identified by using ELISA kit. As a result, intensities of TNF-α, IL-1β, and IL-6 ($P<0.01$) in serum were suggestively augmented by CCl$_4$-induced, while overproduction of TNF-α, IL-1β, and IL-6 were meaningfully repressed by TAX treatment ($P<0.05$; Figure 4A–C). Importantly, immunohistochemical staining was done to examine the anti-inflammatory properties of TAX and to examine the countenance intensities of iNOS and COX-2 in liver tissue. As shown in Figure 4D–F, the positive staining of
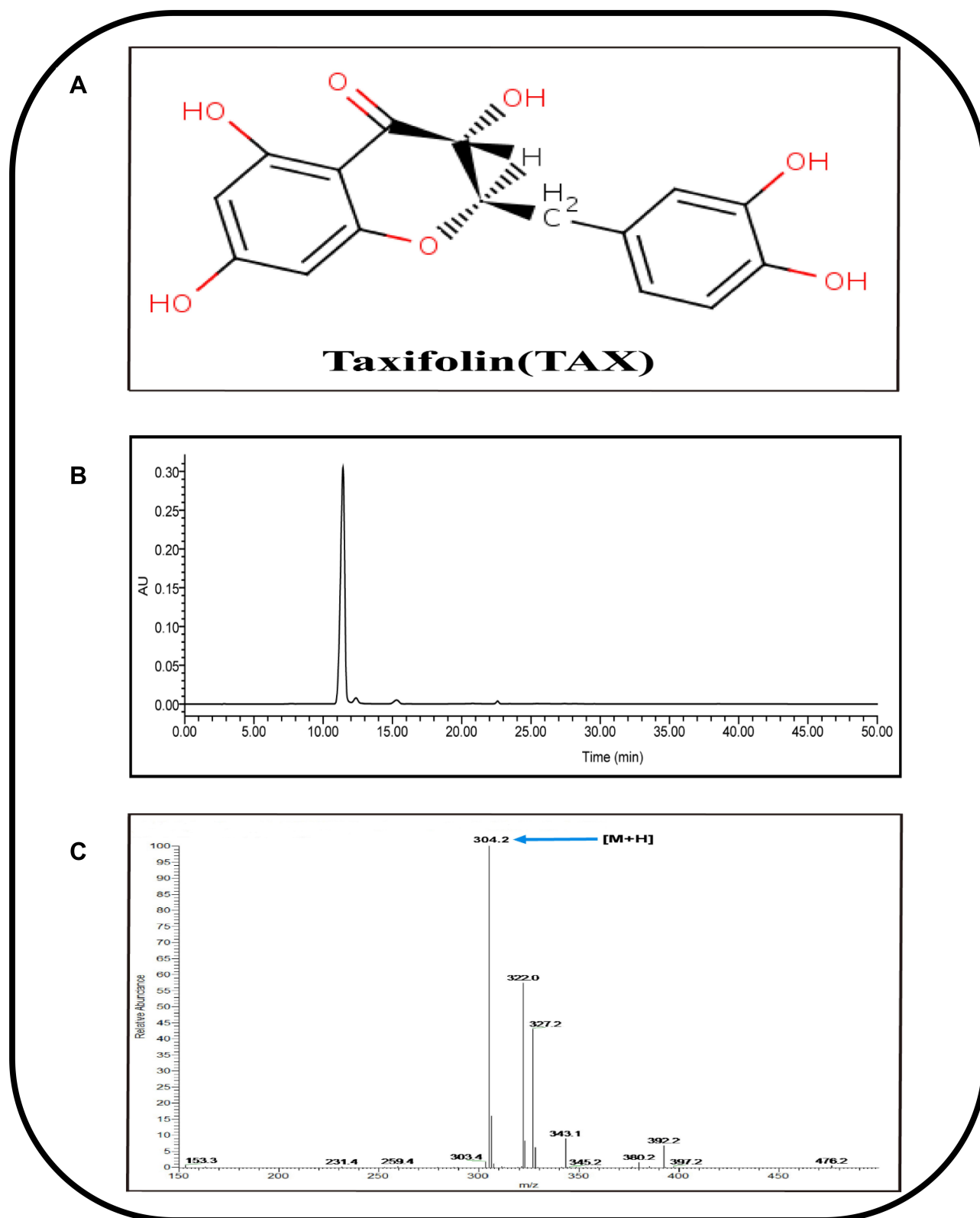
Figure 2 Determination of taxifolin by HPLC-UV/ESI-MS. (**A**) The structure of (2R, 3R)–taxifolin. (**B**) Detection of taxifolin by HPLC-UV. (**C**) The product ion (ESI-MS) spectrum of taxifolin.
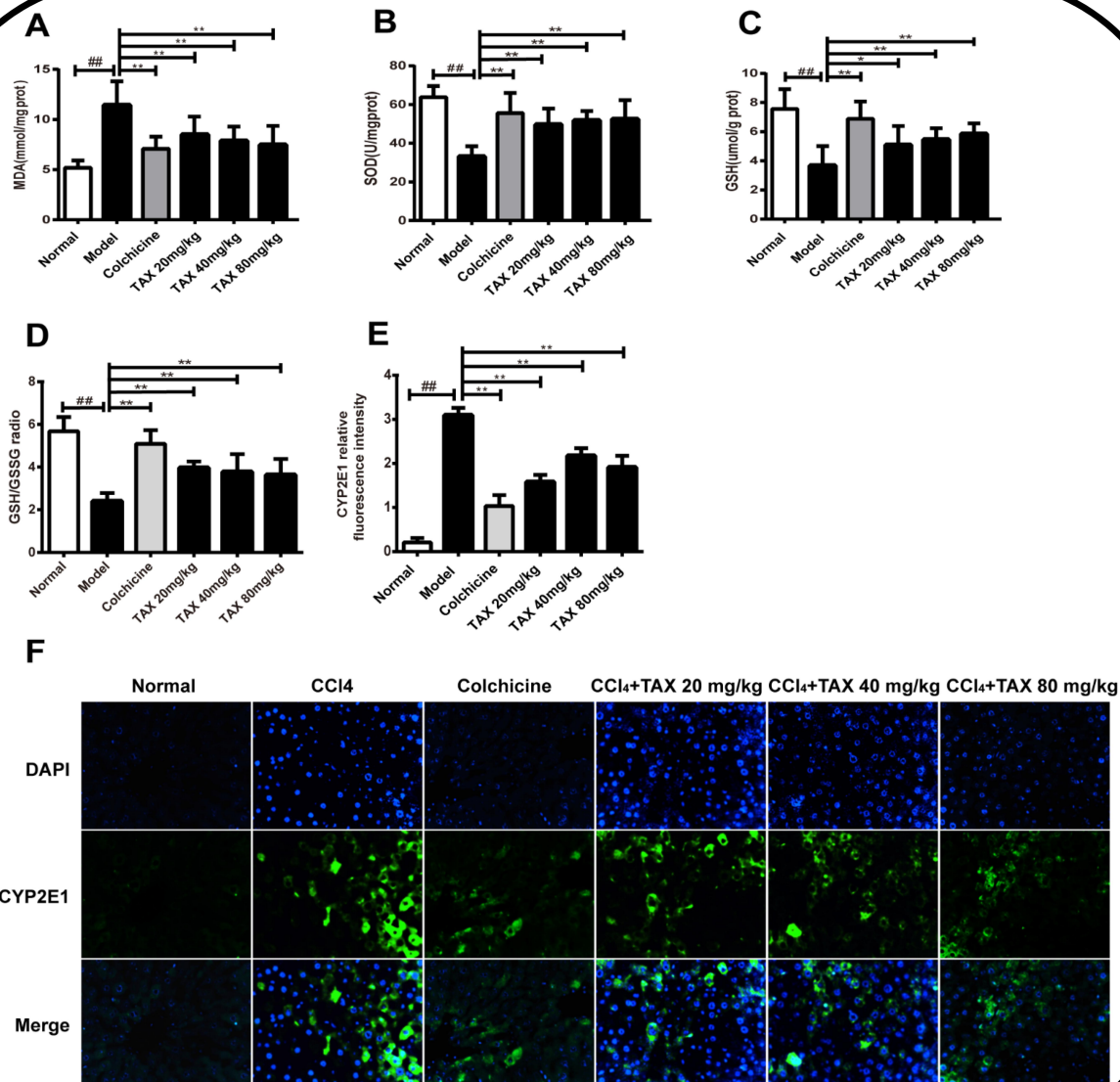
Figure 3 TAX-treatment attenuates CCl₄-induced oxidative stress. (**A**) Lipid peroxidation MDA. (**B**) level of Antioxidant enzyme SOD. (**C**) GSH activities of mice liver. (**D**) GSH/GSSG ratios; (**E** and **F**) Effects of AFG on expressions of CYP2E1 in liver tissue of mice with liver fibrosis and the CYP2E1 relative fluorescence intensity. Representative immunofluorescence images (green) were taken at 200×, 6-Diamidino-2-phenylindole (DAPI) (Blue) acted as a nuclear counterstain. Data are presented as the mean±SD (n=10). As compared with the normal group, $^{\#}P<0.05$ indicates a significant difference, $^{\#\#}P<0.01$ indicates a extremely significant difference; As compared with the model group, $^{*}P<0.05$ indicates a significant difference, $^{**}P<0.01$ indicates an extremely significant difference.
Abbreviations: GSH, glutathione; SOD, superoxide dismutase; MDA, malondialdehyde; CYP2E1, cytochrome P450 E1.

iNOS and COX-2 in the cytoplasmic region of the liver of the model group was noteworthy. However, the countenance of iNOS and COX-2 were lessened by the treatment of TAX in liver tissue at doses of 20, 40, and 80 mg/kg. Therefore, TAX shielded against CCl₄-induced liver fibrosis by reducing oxidative stress and inflammation.

TAX Attenuates CCl₄-Induced Hepatocyte Apoptosis

To investigate the contrivance of the anti-apoptotic effect of TAX, TUNEL staining was done to inspect and calculate the apoptotic hepatocytes. This indicates that apoptosis is consonant with inflammatory necrosis after1 CCl₄-induced. It
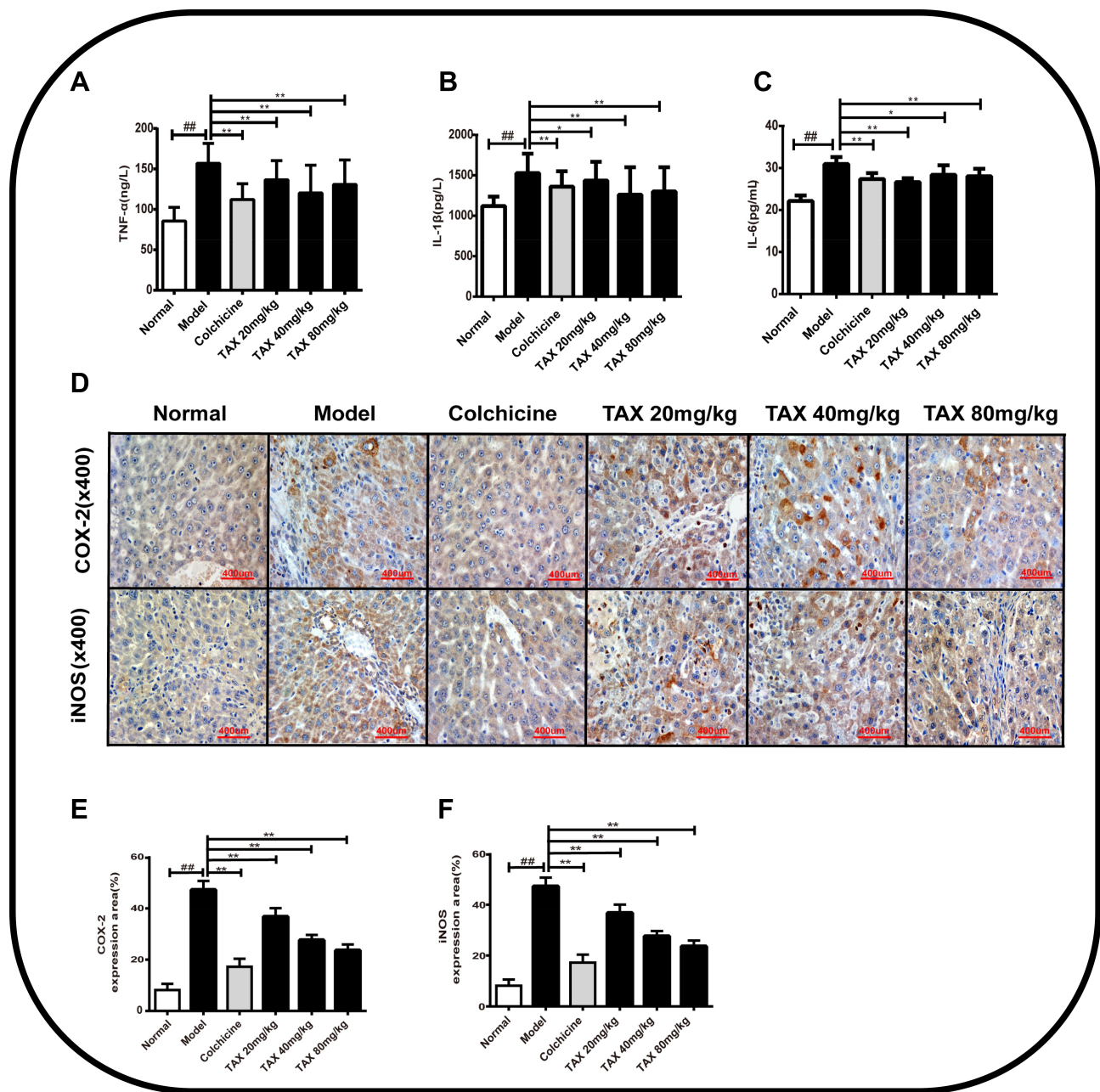
Figure 4 TAX-treatment attenuates CCl₄-induced inflammation injury. (**A–C**) TAX effect on countenance of TNF-α, IL-1β, and IL-6 in mice serum. (**D**) Immunohistochemical staining of COX-2 and iNOS inflammatory factors in liver tissue. (**E** and **F**) Inflammatory cell expression area $^{\%}$Data are presented as the mean ±SD (n=10). As compared with the normal group, $^{\#}P$<0.05 indicates a significant difference, $^{\#\#}P$<0.01 indicates a extremely significant difference; As compared with the model group, $^{*}P$<0.05 indicates a significant difference, $^{**}P$<0.01 indicates an extremely significant difference.
Abbreviations: TNF-α, tumor necrosis factor-α; IL-1β, interleukin-1β; IL-6, interleukin-6; iNOS, inducible nitric oxide synthetase; COX-2, cyclooxygenase-2.

was concluded from the results that apoptosis was not observed in the liver sections of the normal group by TUNEL staining (Figure 5E and F). Compared with the normal group, apoptosis was meaningfully elevated in the liver tissues of the model group (*P*<0.01). However, TAX treatment suggestively lessened the number of apoptotic cells in the liver tissues. The above data indicate that TAX significantly inhibited CCl₄-induced hepatocyte apoptosis

against liver fibrosis. Additionally, countenance intensities of proteins Bax, Bcl-2, caspase-3, and cleaved caspase-3 were scrutinized by Western blotting in order to further observe the TAX activity on CCl₄-induced apoptosis. The level of Bax and cleaved caspase-3 was knowingly increased, as summarized in Figure 5A–D, and Bcl-2 attenuated in the model group (*P*< 0.05). However, compared with the model group, TAX treatment reduced the level of Bax and cleaved
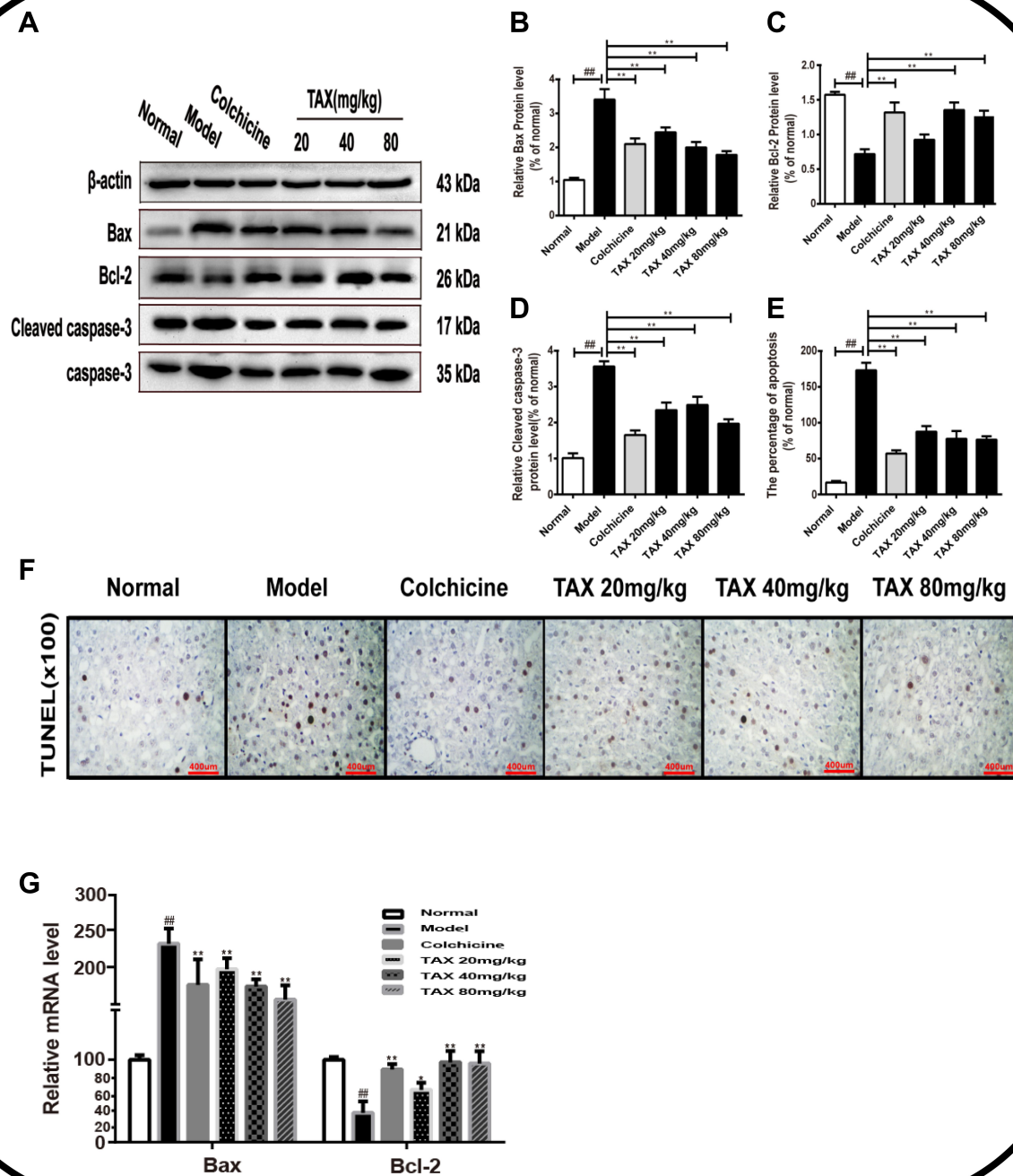
Figure 5 TAX attenuates CCl₄-induced hepatocyte apoptosis. (**A**) Expression of Bcl-2, Bax, and Cleaved caspase-3 in liver tissue by Western blotting; (**B–D**) Densitometric exploration of Western blots; (**E** and **F**) TUNEL staining for counting apoptotic cells and the percentage of apoptosis in liver tissues (%); (**G**) Relative mRNA level of BAX and Bcl-2. Data presented as the mean±SD (n=10). As compared with the normal group, [#]$P<0.05$ indicates a significant difference, [##]$P<0.01$ indicates an extremely significant difference; As compared with the model group, *$P<0.05$ indicates a significant difference, **$P<0.01$ indicates an extremely significant difference.

caspase-3, and improved countenance intensity of Bcl-2, thus adjusting the Bcl-2/Bax proportion, but the caspase-3 level was not significantly different among all groups. The results of Bax and Bcl-2 by rt-PCR analysis were consistent with Western blotting (Figure 5G).

TAX Inhibits HSC Activation by Regulating the TGF-β1/Smads Pathway

To further inspect the progression of liver fibrosis in mice, the HSCs activation is an important marker, thence the collagen deposition, HSCs activation marker α-SMA, and pro-fibrotic

factor TGF-β1 were measured. Various signaling pathways delimited the stimulation and propagation of HSCs. Therefore, the treatment strategy to avoid HSCs activation is considered to be the most effective anti-fibrotic therapy. TGF-β1 is one of the most basic fibrogenic factors, and we inspect it by using an ELISA assay. CCl₄-induced increased in TGF-β1 in the serum of the model group as compared to the control group (*P*<0.01). However, TAX treatment successfully reversed the upsurge (*P*<0.01) equated to the model group (Figure 6B). In addition, α-SMA is a marker of hepatic stellate

cell activation, and Western blotting was done to assess the countenance levels of TGF-β1, Smad3, and α-SMA proteins. The results showed TAX handling may increase the expression of TGF-β1, Smad3, and α-SMA (Figure 6A, C–E), and confirmed that HSCs activated in CCl₄-induced liver fibrosis in mice, and observed consequence was statistically significant (*P*<0.01), which also confirmed that persistent activation of TGF-β1 caused by overexpression of Smad3 resulted in increased liver fibrosis. Interestingly, TAX treatment adjusted these levels (*P*<0.05). In addition, by using rt-PCR the
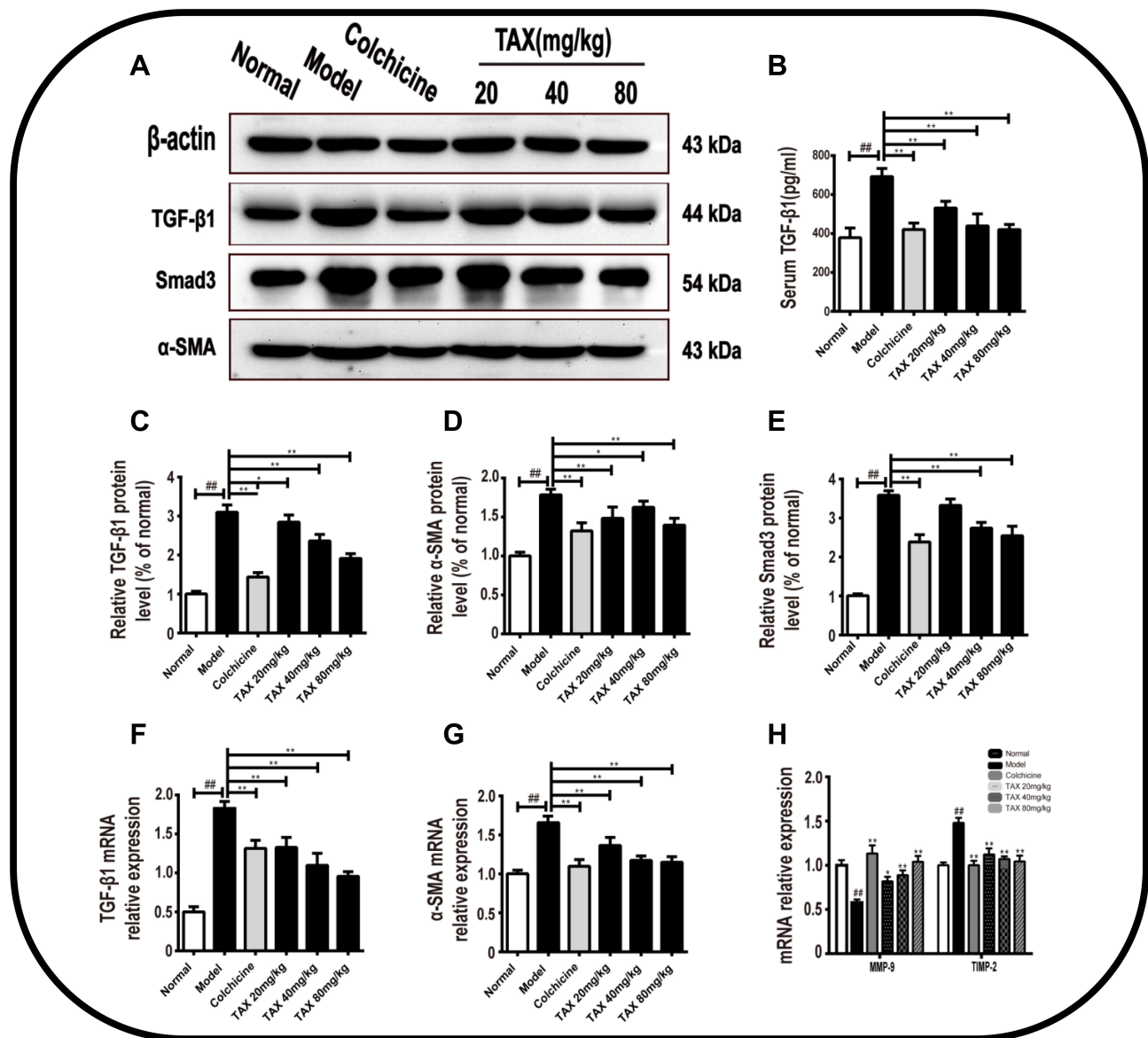

Figure 6 TAX inhibits HSCs activation by regulating TGF-β1/Smads pathway. (**A**) TAX effect on the expression of α-SMA, TGF-β1, Smad3, and β-actin in mice liver were evaluated by Western blotting; (**B**) TGF-β1 (pg/mL) in serum; (**C–E**) Densitometric exploration of Western blotting; (**F–H**) Relative mRNA intensities of α-SMA, TGF-β1, MMP-9, and TIMP-2. Data explored as the mean±SD (n=10). As compared with the normal group, #*P*<0.05 indicates a significant difference, ##*P*<0.01 indicates an extremely significant difference; As compared with the model group, *P*<0.05 indicates a significant difference, **P*<0.01 indicates an extremely significant difference.
Abbreviations: TGF-β1, transforming growth factor-β1; α-SMA, α-smooth muscle actin; ECM, extracellular matrix; HSCs, hepatic stellate cells.

countenance of TGF-β1, α-SMA in the liver were examined (Figure 6F and G), TAX treatment knowingly lessens the countenance of TGF-β1 and α-SMA mRNA (*P*<0.05), and inhibits HSCs activation. Furthermore, we also inspected the effects of TAX on matrix metalloproteinase-9 (MMP-9) and tissue inhibitor of metalloproteinase-2 (TIMP-2) expression levels. We found that TIMP-2 mRNA countenance intensities was meaningfully lesser in the TAX treated group equated to the model group, and the MMP-9 level is knowingly greater than the model group (*P*<0.05; Figure 6H). This study suggested that TAX lessened liver fibrosis by constraining HSCs activation by moderating the TGF-β1/Smads pathway.

TAX Attenuates the PI3K/AKT/mTOR Signaling Pathway in CCl₄-Induced Liver Fibrosis

Furthermore, the PI3K/AKT/mTOR pathway shows an important part in HSCs activation and ECM production in the course of liver fibrosis, thence for exploring the molecular mechanism of TAX against liver fibrosis by CCl₄-induced, the metabolic pathway of PI3K/Akt/mTOR signaling pathway was investigated. As shown in Figure 7A–D, the ratio of p-PI3K/PI3K, p-Akt/Akt, and p-mTOR/mTOR were meaningfully suppressed in the model group equated with the normal group (*P*<0.01). However, the PI3K/AKT/mTOR signaling
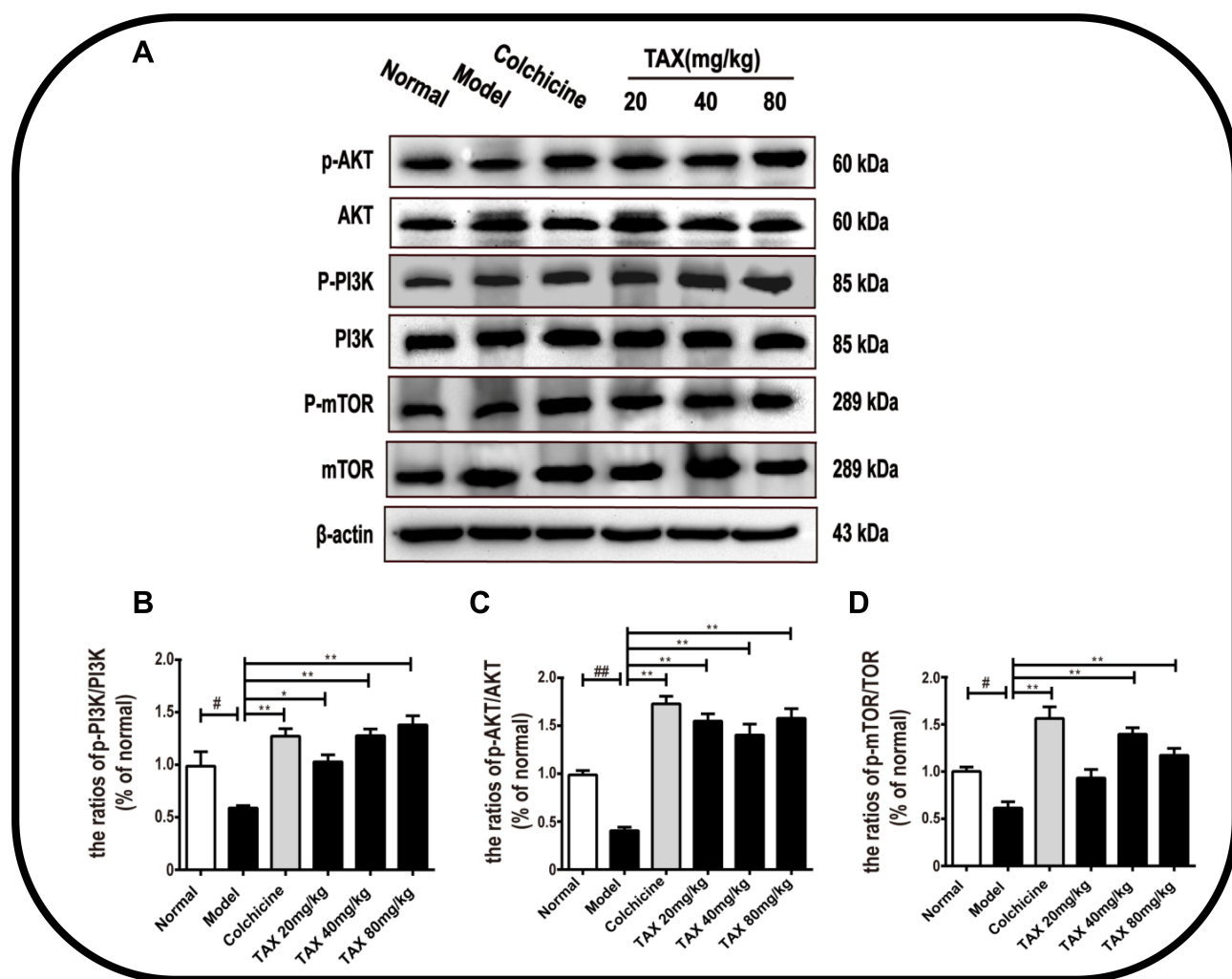

Figure 7 TAX attenuates PI3K/AKT/mTOR signaling pathways in CCl₄-induced liver fibrosis. (**A**) TAX effects on the countenance of PI3K/AKT/mTOR in the liver tissues of mice were examined by Western blotting examination. (**B**–**D**) Densitometric exploration of the p-PI3K/PI3K, p-AKT/AKT, and p-mTOR/TOR. Data presented as the mean ±SD (n=10). As compared with the normal group, #*P*<0.05 indicates a significant difference, ##*P*<0.01 indicates an extremely significant difference; As compared with the model group, *P*<0.05 indicates a significant difference, **P*<0.01 indicates an extremely significant difference.
Abbreviations: Akt, protein kinase B; PI3K, phosphatidylinositol 3-kinase; mTOR, mammalian target of rapamycin.

pathway was reversed by TAX handling and raised intensities of p-PI3K, p-AKT, and p-mTOR was overturned ($P<0.05$). These consequences exhibited that TAX improved the liver fibrosis by moderating the PI3K/AKT/mTOR signaling pathway, and constraining HSCs activation and differentiation.

Discussion

In the advancement of liver cirrhosis, liver fibrosis is an important stage, and no operative remedies are accessible to treat it. Hence, it is required to progress new medications for handling liver fibrosis. In this study, we revealed a method to establish human liver fibrosis model in mice and further explored the role of apoptosis and collagen factors in liver fibrosis. Taxifolin (TAX), as a natural active ingredient, has been proven to have potent antioxidant and anti-inflammatory activities.[16,17] Studies have shown that TAX regulated metabolism in the liver, mainly by activating or inhibiting the activity of related enzymes, regulating the expression of related transcription factors, and inducing autophagy. Therefore, it has great potential for the treatment of liver diseases. Based on the results of this study it was proved that the potential protective effect of TAX on oxidative stress, inflammation, and apoptosis in CCl$_4$-induced liver fibrosis.

In particular, the CCl$_4$-induced model demonstrated that inflammatory infiltration in hepatocytes, and the inflammatory injury further lead to hepatocyte apoptosis and liver fibrosis. Based on TAX pharmacological activity, the research explored the healing influence and molecular mechanism of TAX in CCl$_4$-induced liver fibrosis mice. In the evolution of liver fibrosis, HSCs activation performed an important part and is reflected as a main objective for anti-fibrotic treatment.[27,28] Because of the activation of HSCs, the synthesis of extracellular matrix (ECM) and α-SMA increased. In the present study, to assess the consequence of TAX on HSCs activation the countenance level of TGF-β1, Smad3, and α-SMA were perceived, and these results indicated that TAX could reduce CCl$_4$-induced liver fibrosis by reducing the TGF-β1/Smads signaling pathway and limiting HSCs overactivation.

Liver fibrosis is a disease caused by various chronic damage to the liver, and hepatocytes account for the largest proportion in liver tissues and cells, so they are the target of toxic substances in the liver. Currently studies have shown that the PI3K/AKT/mTOR signaling pathway is involved in the regulation of various intercellular functions, such as proliferation, differentiation, and apoptosis,

and hepatocyte apoptosis exists in the liver fibrosis caused by various factors.[29] Therefore, inhibiting hepatocyte apoptosis is of great significance for the treatment of liver fibrosis, and has become a key factor in metabolic regulation in the treatment of liver diseases.[30,31] As a part of the PI3K-Akt pathway, mTOR kinase is usually regarded as a signaling transducer and sensor for immune cell differentiation and metabolism checkpoint, and the activation of mTOR is responsible for many dynamic changes in proliferating activated T-cells.[32] In addition, mTOR combines with several cofactors to form two different complexes (mTORC1 and mTORC2) constituted by key metabolic checkpoints, which are involved in the activation and differentiation of T cells, and its metabolic changes occur throughout the lifecycle of Tcells, and it is also an important regulator of a variety of cell signaling pathways.[33,34] When the signal is received from exterior cytokines, consistent receptors, for instance that of TGF-β1, can be dimerized to activate the AKT signaling cataract through PI3K, which consequently triggers mTOR to motivate transcription of propagation- and activation-related genes.[35,36] The improvement of liver fibrosis is closely related to the PI3K/AKT/mTOR signaling pathway, and activation of the PI3K/AKT/mTOR signaling pathway can promote liver angiogenesis, improve blood supply, remodel the extracellular matrix, regulate liver cell autophagy, and inhibit hepatocytes apoptosis and promote their proliferation. The results of this study observed that PI3K and AKT were activated and phosphorylated after TAX treatment, and further activated the downstream mTOR and increased the level of its protein expression. TAX handling meaningfully improved the intensities of all of these, demonstrating anti-liver fibrosis consequences of TAX and were dependent on reversing of the PI3K/AKT/mTOR signaling pathway, which also means that taxifolin may be involved in the regulation of metabolic checkpoints when regulating the mTOR/PI3K signaling pathway and also provides a new reference for the treatment of liver fibrosis. In fact, numerous readings confirmed that, for the development of liver fibrosis, the proliferation and activation of HSCs, the production of ECM and the apoptosis of hepatocytes were associated with the PI3K/AKT/mTOR pathway.[8,37,38] All these consequences exhibited that, for the treatment liver fibrosis, TAX showed an important potential healing influence. Remarkably, although great progress has been made, the regulatory metabolic network of metabolic checkpoints in cellular metabolic diseases is not fully understood.[39] In conclusion, it is necessary to

more widely explore different metabolic checkpoints and combine them with signal transduction pathways in the future that regulate the metabolism to formulate new immunotherapies that provide the possibility for the regulation and treatment of liver fibrosis and other metabolic diseases.

Moreover, as TAX has antioxidant and anti-inflammatory possessions, hence the healing consequence of TAX contrary to CCl_4-induced liver fibrosis may be documented to these various therapeutic possessions. Combining previously discovered results, CCl_4-induced fibrosis can lead to oxidative imbalance and oxidative

stress damage, and further cause damage to various tissues and cells of the body, and mediate the abnormal expression of various inflammatory signal pathways.[40,41] Redox imbalance can cause cell oxidative stress which lead to a variety of cytotoxicity, and produce biological reaction by-product reactive oxygen species (ROSs), which is also a critical factor leading to many related diseases.[42] Meanwhile, ROS is involved in the destruction of redox regulation mechanism, which is also an important factor leading to disease progression and chemoresistance.[43] Therefore, there is an urgent need to find targeted precise molecular mechanisms to control the balance of ROS,
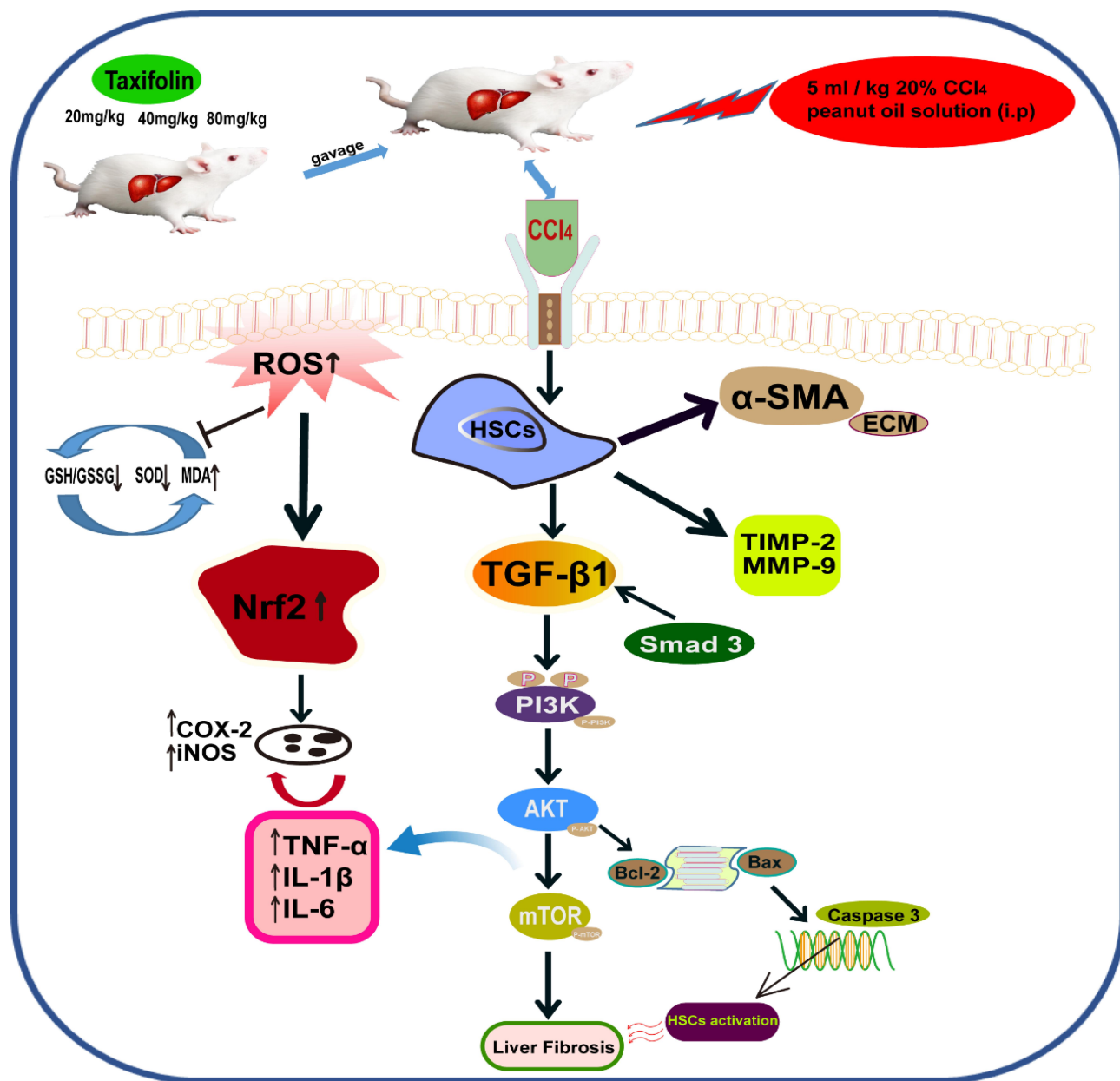

Figure 8 TAX treatment constrains HSCs activation and ECM synthesis via reversing of the PI3K/AKT/mTOR and TGF-β1/Smads signaling pathways.

which may be a potential therapeutic strategy to overcome chemoresistance. Oxidative imbalance is accompanied by the reduced activity of nuclear-related factor 2 (Nrf2) in the body, while NRF2 is a well-known transcriptional master regulator, which is believed to recognize cellular oxidative stress, and then combine with the promoters of cytoprotective and antioxidant genes to promote antioxidant reactions which participate in maintaining the redox state of cells.[44] In addition, as an upstream and downstream regulator, Nrf2 can regulate the transcription of anti-oxidative stress and anti-inflammatory genes, and its activation is one of the main defense mechanisms of cells.[45] The up-regulated Nrf2 signaling pathway inhibits the release of pro-inflammatory cytokines COX-2, IL-6, and TNF-α, improves liver immunity and metabolism, and reduces inflammatory injury and hypofunction. It is worth mentioning that a recent study shows activated Nrf2 regulates sensitivity of PDAC cells (pancreatic ductal adenocarcinomas, PDAC) to gemcitabine and chemoresistance.[46] Therefore, as a major regulator of neutralizing cellular ROS and restoring redox balance, indepth exploration of the role of Nrf2 in ROS-mediated chemoresistance may help to develop therapeutic strategies with higher efficacy. Our research shows that taxifolin, as a natural antioxidant, can alleviate oxidative imbalance and oxidative stress damage caused by a large amount of accumulated ROS, and may be involved in regulating Nrf2 signal transduction and ameliorating chemoresistance to maintain cell function. Although it is still poorly understood if the activation of Nrf2 pathway is involved in the mechanism of chemical resistance in the treatment of liver fibrosis, this evidence at least proves that Nrf2 as a key regulator is involved in chemoresistance, which also has great enlightenment for our future work.

Furthermore, in order to evaluate the consequence of TAX on the inflammatory response, the intensities of inflammatory cytokines and biomarkers were identified by rt-PCR. Our consequences verified that after CCl₄-induction, there were noteworthy elevated intensities of the inflammatory cytokines and biomarkers iNOS, COX-2, TNF-α, IL-6, and IL-1β were meaningfully diminished by TAX-treatment. Apoptosis, a foremost form of cell demise, is synchronized by several molecular signaling pathways counting mitochondrial pathways.[47,48] In these pathways, the family of Bcl-2 proteins is firmly organized by the mitochondrial outer membrane permeabilization.[49–51] In the study, the countenance intensities of caspase-3, cleaved

caspase-3, Bcl-2, and Bax were explored, and the consequences revealed that the intensities of caspase-3, cleaved caspase-3, and Bcl-2 expression were declined, yet Bax was enhanced CCl₄-induced. However, the levels of these apoptotic factors could be reversed by TAX-treatment. Consequently, our results specified that TAX alleviated CCl₄-induced liver fibrosis by preventing hepatocyte apoptosis.

Conclusions

In conclusion, our results confirmed that TAX improves liver fibrosis in mice through numerous mechanisms. First of all, TAX applies a hepatoprotective activity by lessening CCl₄-induced oxidative stress, inflammation, and apoptosis. Additionally, it is further concluded that TAX treatment constrains HSCs activation and ECM synthesis via reversing of the PI3K/AKT/mTOR and TGF-β1/Smads signaling pathways (Figure 8). These consequences propose that TAX has a prospective cure for liver fibrosis and provides a reference for clinical treatment of liver fibrosis in the future.

Acknowledgments

Disclosure

The authors report no conflicts of interest in this work.

References

1. Bataller R, Brenner DA. Liver fibrosis. *J Clin Invest*. 2005;115:209–218. doi:10.1172/JCI24282
2. Eom YW, Shim KY, Baik SK. Mesenchymal stem cell therapy for liver fibrosis. *Korean J Intern Med*. 2015;30:580–589. doi:10.3904/kjim.2015.30.5.580
3. Gao B, Bataller R. Alcoholic liver disease: pathogenesis and new therapeutic targets. *Gastroenterology*. 2011;141:1572–1585. doi:10.1053/j.gastro.2011.09.002
4. Iwaisako K, Jiang C, Zhang M, et al. Origin of myofibroblasts in the fibrotic liver in mice. *Proc Natl Acad Sci USA*. 2014;111:E3297–E3305. doi:10.1073/pnas.1400062111
5. Popov Y, Schuppan D. Targeting liver fibrosis: strategies for development and validation of antifibrotic therapies. *Hepatology*. 2009;50:1294–1306. doi:10.1002/hep.23123
6. Mederacke I, Hsu CC, Troeger JS, et al. Fate tracing reveals hepatic stellate cells as dominant contributors to liver fibrosis independent of its aetiology. *Nat Commun*. 2013;4. doi:10.1038/ncomms3823.

7. Seki E, Schwabe RF. Hepatic inflammation and fibrosis: functional links and key pathways. *Hepatology*. 2015;61:1066–1079. doi:10.1002/hep.27332

8. Son G, Hines IN, Lindquist J, Schrum LW, Rippe RA. Inhibition of phosphatidylinositol 3-kinase signaling in hepatic stellate cells blocks the progression of hepatic fibrosis. *Hepatology*. 2009;50:1512–1523. doi:10.1002/hep.23186

9. Xia Tang L, Hua He R, Yang G, et al. Asiatic acid inhibits liver fibrosis by blocking TGF-beta/smad signaling in vivo and in vitro. *PLoS One*. 2012. doi:10.1371/journal.pone.0031350

10. Tian Z, Greene AS, Pietrusz JL, Matus IR, Liang M. MicroRNA-target pairs in the rat kidney identified by microRNA microarray, proteomic, and bioinformatic analysis. *Genome Res*. 2008;18:404–411. doi:10.1101/gr.6587008

11. Guicciardi ME, Gores GJ. Apoptosis as a mechanism for liver disease progression. *Semin Liver Dis*. 2010;30:402–410. doi:10.1055/s-0030-1267540

12. Wang R, Zhang H, Wang Y, Song F, Yuan Y. Inhibitory effects of quercetin on the progression of liver fibrosis through the regulation of NF-κB/IκBα, p38 MAPK, and Bcl-2/Bax signaling. *Int Immunopharmacol*. 2017;47:126–133. doi:10.1016/j.intimp.2017.03.029

13. Anu SM, Kim HJ, Kim JE, Boo YC. Flavonoids, taxifolin and luteolin attenuate cellular melanogenesis despite increasing tyrosinase protein levels. *Phytother Res*. 2008;22:1200–1207. doi:10.1002/ptr.2435

14. Yang P, Xu F, Li HF, et al. Detection of taxifolin metabolites and their distribution in rats using HPLC-ESI-IT-TOF-MSn. *Molecules*. 2016. doi:10.3390/molecules21091209

15. Wang Y, Zu Y, Long J, et al. Enzymatic water extraction of taxifolin from wood sawdust of Larix gmelini (Rupr.) Rupr. and evaluation of its antioxidant activity. *Food Chem*. 2011. doi:10.1016/j.foodchem.2010.11.155

16. Weidmann AE. Dihydroquercetin: more than just an impurity? *Eur J Pharmacol*. 2012;684:19–26. doi:10.1016/j.ejphar.2012.03.035

17. Sugihara N, Arakawa T, Ohnishi M, Furuno K. Anti- and pro-oxidative effects of flavonoids on metal-induced lipid hydroperoxide-dependent lipid peroxidation in cultured hepatocytes loaded with α-linolenic acid. *Free Radic Biol Med*. 1999;27:1313–1323. doi:10.1016/S0891-5849(99)00167-7

18. Chu SC, Hsieh YS, Lin JY. Inhibitory effects of flavonoids on moloney murine leukemia virus reverse transcriptase activity. *J Nat Prod*. 1992;55:179–183. doi:10.1021/np50080a005

19. Romero MR, Serrano MA, Efferth T, Alvarez M, Marin JJG. Effect of cantharidin, cephalotaxine and homoharringtonine on "in vitro" models of Hepatitis B Virus (HBV) and Bovine Viral Diarrhoea Virus (BVDV) replication. *Planta Med*. 2007;73:552–558. doi:10.1055/s-2007-967184

20. Kandaswami C, Perkins E, Drzewiecki G, Soloniuk DS, Middleton E. Differential inhibition of proliferation of human squamous cell carcinoma, gliosarcoma and embryonic fibroblast-like lung cells in culture by plant flavonoids. *Anticancer Drugs*. 1992;3:525–530. doi:10.1097/00001813-199210000-00013

21. Devi MA, Das NP. In vitro effects of natural plant polyphenols on the proliferation of normal and abnormal human lymphocytes and their secretions of interleukin-2. *Cancer Lett*. 1993;69:191–196. doi:10.1016/0304-3835(93)90174-8

22. Kawaii S, Tomono Y, Katase E, Ogawa K, Yano M. Effect of citrus flavonoids on HL-60 cell differentiation. *Anticancer Res*. 1999.

23. Sun X, Chang Chen R, Hong Yang Z, et al. Taxifolin prevents diabetic cardiomyopathy in vivo and in vitro by inhibition of oxidative stress and cell apoptosis. *Food Chem Toxicol*. 2014. doi:10.1016/j.fct.2013.11.013

24. Guo H, Zhang X, Cui Y, et al. Taxifolin protects against cardiac hypertrophy and fibrosis during biomechanical stress of pressure overload. *Toxicol Appl Pharmacol*. 2015;287:168–177. doi:10.1016/j.taap.2015.06.002

25. Rogovskii VS, Matyushin AI, Shimanovskii NL, et al. Antiproliferative and antioxidant activity of new dihydroquercetin derivatives. *Eksp I Klin Farmakol*. 2010. doi:10.30906/0869-2092-2010-73-9-39-42

26. Poli G. Pathogenesis of liver fibrosis: role of oxidative stress. *Mol Aspects Med*. 2000;21:49–98. doi:10.1016/S0098-2997(00)00004-2

27. Friedman SL. Mechanisms of Hepatic Fibrogenesis. *Gastroenterology*. 2008;134:1655–1669. doi:10.1053/j.gastro.2008.03.003

28. Seki E, Brenner DA. Recent advancement of molecular mechanisms of liver fibrosis. *J Hepatobiliary Pancreat Sci*. 2015;22:512–518. doi:10.1002/jhbp.245

29. Ibusuki R, Uto H, Oda K, et al. Human neutrophil peptide-1 promotes alcohol-induced hepatic fibrosis and hepatocyte apoptosis. *PLoS One*. 2017;12:e0174913. doi:10.1371/journal.pone.0174913

30. Paul D. New methods to control neuroblastoma growth. *Cancer Biol Ther*. 2014. doi:10.4161/cbt.28465

31. Zhai B, Hu F, Jiang X. Inhibition of Akt reverses the acquired resistance to sorafenib by switching protective autophagy to autophagic cell death in hepatocellular carcinoma. *Mol Cancer Ther*. 2014;13:1589–1598. doi:10.1158/1535-7163.MCT-13-1043

32. Roy S, Rizvi ZA, Awasthi A. Metabolic checkpoints in differentiation of helper T cells in tissue inflammation. *Front Immunol*. 2019;9. doi:10.3389/fimmu.2018.03036.

33. Mukhopadhyay S, Saqcena M, Foster DA. Synthetic lethality in KRas-driven cancer cells created by glutamine deprivation. *Oncoscience*. 2015;2:807–808. doi:10.18632/oncoscience.253

34. Feng F-B, Qiu HY. Effects of Artesunate on chondrocyte proliferation, apoptosis and autophagy through the PI3K/AKT/mTOR signaling pathway in rat models with rheumatoid arthritis. *Biomed Pharmacother*. 2018;102:1209–1220. doi:10.1016/j.biopha.2018.03.142

35. Engelman JA. Targeting PI3K signalling in cancer: opportunities, challenges and limitations. *Nat Rev Cancer*. 2009;9:550–562. doi:10.1038/nrc2664

36. Polivka J, Janku F. Molecular targets for cancer therapy in the PI3K/AKT/mTOR pathway. *Pharmacol Ther*. 2014;142:164–175. doi:10.1016/j.pharmthera.2013.12.004

37. Urtasun R, Lopategi A, George J, et al. Osteopontin, an oxidant stress sensitive cytokine, up-regulates collagen-I via integrin α Vβ 3 engagement and PI3K/pAkt/NFκB signaling. *Hepatology*. 2012;55:594–608. doi:10.1002/hep.24701

38. Peng R, Yuan Y. Antifibrotic effects of tanshinol in experimental hepatic fibrosis by targeting PI3K/AKT/mTOR/p70S6K1 signaling pathways. *Discov Med*. 2017.

39. Shevchenko I, Bazhin AV. Metabolic checkpoints: novel avenues for immunotherapy of cancer. *Front Immunol*. 2018;9. doi:10.3389/fimmu.2018.01816.

40. Brenner C, Galluzzi L, Kepp O, Kroemer G. Decoding cell death signals in liver inflammation. *J Hepatol*. 2013;59:583–594. doi:10.1016/j.jhep.2013.03.033

41. Luedde T, Kaplowitz N, Schwabe RF. Cell death and cell death responses in liver disease: mechanisms and clinical relevance. *Gastroenterology*. 2014;147:765–783.e4. doi:10.1053/j.gastro.2014.07.018

42. Fallah A, Sadeghinia A, Kahroba H, et al. Therapeutic targeting of angiogenesis molecular pathways in angiogenesis-dependent diseases. *Biomed Pharmacother*. 2019;110:775–785. doi:10.1016/J.BIOPHA.2018.12.022

43. Xue D, Zhou X, Qiu J. Emerging role of NRF2 in ROS-mediated tumor chemoresistance. *Biomed Pharmacother*. 2020;131:110676. doi:10.1016/j.biopha.2020.110676

44. Payandeh Z, Tazehkand AP, Barati G, et al. Role of Nrf2 and mitochondria in cancer stem cells; in carcinogenesis, tumor progression, and chemoresistance. *Biochimie*. 2020;179:32–45. doi:10.1016/j.biochi.2020.09.014

45. Kalkavan H, Green DR. MOMP, cell suicide as a BCL-2 family business. *Cell Death Differ*. 2018;25:46–55. doi:10.1038/cdd.2017.179

46. Mukhopadhyay S, Goswami D, Adiseshaiah PP, et al. Undermining glutaminolysis bolsters chemotherapy while NRF2 promotes chemoresistance in KRAS-driven pancreatic cancers. *Cancer Res*. 2020;80:1630–1643. doi:10.1158/0008-5472.can-19-1363

47. Yuan R, Huang L, Du L. Dihydrotanshinone exhibits an anti-inflammatory effect in vitro and in vivo through blocking TLR4 dimerization. *Pharm Res*. 2019;142:102–114. doi:10.1016/j.phrs.2019.02.017

48. Lee I, Yang C. Role of NADPH oxidase/ROS in proinflammatory mediators-induced airway and pulmonary diseases. *Biochem Pharmacol*. 2012;84:581–590. doi:10.1016/j.bcp.2012.05.005

49. Steel R, Cowan J, Payerne E, O'Connell MA, Searcey M. Anti-inflammatory effect of a cell-penetrating peptide targeting the Nrf2/Keap1 interaction. *ACS Med Chem Lett*. 2012;3:407–410. doi:10.1021/ml300041g

50. Benyon RC, Arthur MJP. Extracellular matrix degradation and the role of hepatic stellate cells, Semin. *Semin Liver Dis*. 2001;21:373–384. doi:10.1055/s-2001-17552

51. Kim DC, Jun DW, Kwon Y, et al. 5-HT 2A receptor antagonists inhibit hepatic stellate cell activation and facilitate apoptosis. *Liver Int*. 2013;33:535–543. doi:10.1111/liv.12110